Classification Model of Wireless Signals Based on Higher-order Statistics

Fangning Shi[1]
Key Laboratory of Trustworthy Distributed Computing and Service (BUPT) Ministry of Education
Beijing University of Posts and Telecommunications
Beijing, China
2019110120sfn@bupt.edu.cn

Xiaojun Jing[1]
Key Laboratory of Trustworthy Distributed Computing and Service (BUPT) Ministry of Education
Beijing University of Posts and Telecommunications
Beijing, China
jxiaojun@bupt.edu.cn

Yuan He[1]
Key Laboratory of Trustworthy Distributed Computing and Service (BUPT) Ministry of Education
Beijing University of Posts and Telecommunications
Beijing, China
yuanhe@bupt.edu.cn

Michel Kadoch[2]
ETS
University of Quebec
Montreal,Canada
michel.kadoch@etsmtl

Mohamed Cheriet[2]
ETS
University of Quebec
Montreal,Canada
mohamed.cheriet@etsmtl

***Abstract*—Automatic modulation classification technology is an indispensable step in cognitive radio, and its recognition accuracy is related to the orderly progress of subsequent communications. In this paper, we introduce the higher-order statistics into residual neural network for the precise classification of different modulation types. The classification technology can recognize 24 digital and analog modulation types under both synthetic simulated channel effects and over-the-air recordings. We also consider a rigorous baseline method using residual neural network and compare performance between two approaches under a wide range of signal-to-noise ratio. Experimental results show that our proposed method achieves an average accuracy of 96.4% and obtains better performance in correct classification probability than the baseline method, especially in lower signal-to-noise ratio.**

Keywords—automatic modulation classification; cognitive radio; the higher-order statistics; residual neural network, simulated channel effects

I. Introduction

Recently, high-order modulation technology is widely used in wireless communication for its higher data transmission rate and frequency utilization rate, which makes it necessary to explore a precise scheme for the automatic modulation classification and recognition of wireless signals. With the rapid development of deep learning technology, more and more deep learning methods have been proposed in image processing to solve problems and achieve good experimental results and successful industrial applications [1]. O'shea et al. [2] introduced deep learning methods to the field of cognitive radio, bringing an intelligent engine to cognitive radio and making signal recognition becomes an end-to-end process.

In the field of wireless signal classification and recognition, traditional approaches can be categorized into maximum-likelihood based (LB) and feature-based (FB) methods [3]. The practical realization of ML-based AMC is difficult for its high computational complexity and the manually extracted features require abundant prior knowledge, while the feature-based learning is more widely used for its robust performance and low complexity by feature extraction methods. Various types of feature have been proposed [4]-[6], such as time-frequency distributions, constellation diagram and high-order statistics. However, no universal features with better properties have been found to serve as inputs for automatic classification. Besides, the classification performance of network for QAMs was poor. Moreover, these existing methods were mostly developed and optimized for additive white Gaussian noise (AWGN) environments, while these methods suffer from performance degradation in real propagation effects. More and more researchers improve the classifier's performance by converting formation of signal data or proposing new deep neural networks. Wang et al. [5] solved this problem by applying a combination of two CNNs and two formations of inputs to distinguish 16 quadratic-amplitude modulation (QAM) and 64 QAM.

In this study, a novel automatic classification method is designed to classify 24 modulation types under real propagation effects, which leverages the robust performance of higher-order statistics. Compared with traditional convolutional neural networks, our proposed model no longer relies on convolutional layers to extract potential feature parameters from the received signals in a noisy environment. Besides, by considering mathematical theory of modulation, we apply statistical methods to calculate feature quantities, which utilize the higher-statistics to distinguish specific features of different received signals. The selected higher-order statistics were based on the analysis of empirical distributions for each modulation type. Since feature extraction process is one of the most important processes in AMC scheme, accordingly, extracted feature quantities consist of ResNet potential feature parameters and higher-order statistical features in the time domain. As a classifier, the softmax layer at the output layer produces the probability of each modulation type at each code. For successful training of the network, we respectively normalize the high dimensional feature vectors and then concatenate before feeding into the full connection layer. Even though the effect of real propagation scenarios, we see that our proposed model offers good performance under a wide range of SNR and achieves an overall classification accuracy over 95%.

The rest of this paper is organized as follows. In Section II, we introduce the network structure and the higher-order statistics used for our proposed scheme. In Section IV, we discuss the experimental results, and finally in Section V we summarize the paper.

2020 IEEE International Symposium on Broadband Multimedia Systems and Broadcasting (BMSB) | 978-1-7281-5784-9/20/$31.00 ©2020 IEEE | DOI: 10.1109/BMSB49480.2020.9379916

978-1-7281-5784-9/19/$31.00 ©2019 IEEE

Authorized licensed use limited to: INSTITUTO MILITAR DE ENGENHARIA. Downloaded on April 12,2025 at 16:59:36 UTC from IEEE Xplore. Restrictions apply.

II. HOS-BASED MODULATION CLASSIFICATION

In this section, the main work of this paper is exhibited. Firstly, structure of our proposed model is detailed. And the higher-order statistics we utilized in our model is analyzed.

A. Deepsig Dataset

We use a public dataset RadioML2018.10a, which has been heavily validated [2]. Different from other datasets, this public dataset consists of twenty-four modulation types, which are captured under impaired channel environments and over-the-air recordings. Note that the synthetic simulated channel applies a series of impairments, such as the carrier frequency offset, symbol rate offset, and delay spread, which are more than the effect of additive white Gaussian noise.

The twenty-four different analog and digital modulators cover a wide range of single-carrier modulation schemes, which include OOK, 4ASK, 8ASK, BPSK, QPSK, 8PSK, 16PSK, 32PSK, 16APSK, 32APSK, 64APSK, 128APSK, 16QAM, 32QAM, 64QAM, 128QAM, 256QAM, AM-SSB-WC, AM-SSB-SC, AM-DSB-WC, AM-DSB-SC, FM, GMSK, OQPSK. We find that these twenty-four modulation types are widely used in real wireless communication environments.

B. Proposed model

Our system is designed to recognize 24 modulation types under synthetic simulated channel effects and over-the-air recordings. The illustrative structure of our model is shown in Fig. 1.

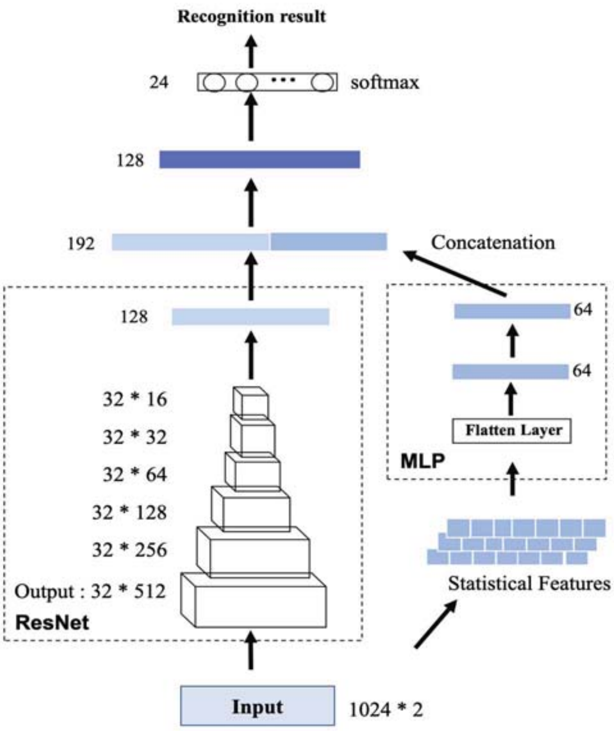

Fig. 1 The structure of HoS-based ResNet

Of significant note here, the inputs of our model are raw samples of each wireless signal example which have been normalized to unit variance. Next, feature extraction part is one of the improvements in our model. Considering higher-order statistical feature quantities are not significantly impacted by the presence of time-varying impairments and short-time observations, it's chosen as the characteristic parameters to extract feature. And then, the statistical features are fed into multilayer perceptron, which is a potent function approximator to abstract feature. The number of its nodes at each layer is specified in Fig. 1. Additionally, the residual unit and residual stack is shown in Fig. 2, each residual unit in ResNet is realized by the skip connection of input parameters and convolution layers' output, and then activated by rectified linear unit (ReLU). The other feature extraction is implemented by stacking of residual unit, linear convolution layer, and max-pooling layer. Therefore, in this paper, the feature maps are obtained from concatenating two different feature vectors, which are respectively generated from the residual stacks and multilayer perceptron. Especially, in this part, we should ensure that the measurement units of each feature parameter of samples are the same and the value of feature parameter of samples fit to the probability distribution, i.e. [0,1] before concatenation. This step is designed to help our model converge at the beginning of training.

After concatenating the normalized feature vectors, the output vectors are squeezed into a vector by a flatten layer. Then a dense layer encodes the output of former layer into vectors which contain higher-level information. Finally, the recognition result is produced by the dense layer with activation function softmax.

In this paper, we choose ResNet from [2] as baseline model, because ResNet shows significant improvement for operating at multiple scales and depths through the skip-connection network; any further improvements should be considered state of the art.

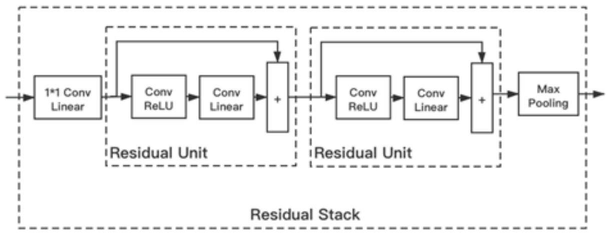

Fig. 2 The basic residual stack of ResNet

During the training process, we apply some tricks to accelerate model convergence and prevent overfitting. The direct training of HoS-based model is challenging with the difficult dataset and complicated model, so pre-trained parameters of baseline method are introduced as the backbone network to improve the efficiency of training. We employ batch normalization to adjust the data distribution so that the output of each layer is normalized to a distribution with a mean value of 0 and a variance of 1, which ensures the effectiveness of the gradient and speeds up the training. We also utilize global max-pooling over feature maps in each residual stack, which is easier to interpret and less prone to overfitting than traditional fully connected layers. In addition, the categorical cross-entropy is adopted as loss function, minimized by the stochastic gradient descent (SGD) algorithm. the rectified linear unit (ReLU) is selected as the activation function for all available layers except the last fully connected layer, where softmax is applied to obtain the

Authorized licensed use limited to: INSTITUTO MILITAR DE ENGENHARIA. Downloaded on April 12,2025 at 16:59:36 UTC from IEEE Xplore. Restrictions apply.

probability distribution matrix of the last layer and dropout operation is used in this case to avoid overfitting.

The detailed process of our proposed structure can be described by algorithm 1, where Fea_1 and Fea_2 respectively refers to the ResNet-based representation feature and HoS-based statistical feature.

Algorithm 1 The proposed network structure

Require: Raw signal data

Ensure: recognition results

1: $Fea_1^{'} \leftarrow$ Normalized Fea_1

2: $Fea_2^{'} \leftarrow$ Normalized Fea_2

3: $Fea^{'}=[Fea_1^{'},Fea_2^{'}] \leftarrow$ Serial Concatenation

4: [Test_fea, Train_fea]$\leftarrow Fea^{'}$

5: Map the high dimensional feature vectors to dense layer

6: Find the optimal hyperparameters $\leftarrow$ parameter optimization

7: **return** Categories

C. Higher-order Statistics Analysis

Under the effects of time-varying channel impairments, we explore using the statistical method to obtain statistical features of each modulation types. Primarily, in this paper, the received data can be expressed as follows:

$$r[i]=r_I[i]+jr_Q[i] \tag{1}$$

where r[i] represents the i-th signal sample, $r_I[i]$ and $r_Q[i]$ represent the in-phase and quadrature part of r[i], respectively.

Higher-order statistics have been widely utilized in literature for having stable performance and showing sensitivity to small changes under the presence of carrier phase and frequency offset in low signal-to-noise ratio, comparing to other features. To obtain the higher order moments, we use expressions given below:

$$M_{p+q,p}=E[(r[i])^p(r[i]^*)^q] \tag{2}$$

where “*” represents complex conjugate, E[·] is expectation.

The high order cumulants are represented by C_{pq} and can be computed combinatorically using high order moments. The considered cumulants in this paper are shown in Table I:

TABLE I. THE EXPRESSIONS OF HIGH ORDER CUMULANTS

HOCs		*HOMs expressions*
4-th order cumulants	C_{40}	M_{40}-$3M_{20}^2$
	C_{42}	M_{42}-M_{20}^2-$2M_{21}^2$
6-th order cumulants	C_{60}	M_{60}-$15M_{20}M_{40}$+$30M_{20}^3$
	C_{61}	M_{61}-$5M_{21}M_{40}$-$10M_{20}M_{41}$+$30M_{20}^2M_{21}$
	C_{62}	M_{62}-$6M_{20}M_{42}$-$8M_{21}M_{41}$-$M_{22}M_{40}$+$6M_{20}^2M_{22}$+$24M_{21}^2M_{20}$
	C_{63}	M_{63}-$9M_{21}M_{42}$+$12M_{21}^3$-$3M_{20}M_{43}$-$3M_{22}M_{41}$+$18M_{20}M_{21}M_{22}$

Due to higher order cumulants alone cannot perfectly describe the characteristics of random signal, we introduce the standard deviation of normalized instantaneous amplitude and phase with mathematical equations below:

$$\sigma_{aa}=\sqrt{\frac{1}{N}\left(\sum_{i=1}^{N} r_{cn}^2[i]\right)-\left(\frac{1}{N}\sum_{i=1}^{N}|r_{cn}^2[i]|\right)^2} \tag{3}$$

$$\sigma_{af}=\sqrt{\frac{1}{N}\left(\sum_{i=1}^{N} f_N^2[i]\right)-\left(\frac{1}{N}\sum_{i=1}^{N}|f_N^2[i]|\right)^2} \tag{4}$$

$$\sigma_{dp}=\sqrt{\frac{1}{c}\left(\sum_{r_n[i]>r_t} \varphi_{NL}^2[i]\right)-\left(\frac{1}{c}\sum_{r_n[i]>r_t}\varphi_{NL}[i]\right)^2} \tag{5}$$

$$\sigma_{ap}=\sqrt{\frac{1}{c}\left(\sum_{r_n[i]>r_t} \varphi_{NL}^2[i]\right)-\left(\frac{1}{c}\sum_{r_n[i]>r_t}|\varphi_{NL}[i]|\right)^2} \tag{6}$$

where $r_{cn}[i]=\frac{|r[i]|}{m_r}-1$ is the normalized signal samples, $m_r=\frac{1}{N}\sum_{i=1}^{N}|r[i]|$, N is the number of samples used for $r_{cn}[i]$, $\varphi[i]$=phase(r[i]), $\varphi_{NL}[i]=\varphi[i]-\frac{1}{N}\sum_{i=1}^{N}\varphi[i]$ is the centered instantaneous phase at time instant, r_t is the threshold, f[i]=frequency(r[i]), $f_N[i]=(f[i]-\frac{1}{N}\sum_{i=1}^{N}f[i])T_s$ is the centered instantaneous frequency, T_s refers to the sample time, c is the total number of samples.

However, these former characteristics cannot perfectly classify QAMs, , some additional features are needed to get more advantageous feature information and improve the recognition, such as kurtosis (K), skewness (S), peak- to-average ratio (PAR), peak-to-rms ratio (PRR), and maximum value of power spectral density (PSD) of the normalized signal samples, which are defined as below:

$$K=\left|\frac{E[(|r[i]|-m_r)^4]}{E[(|r[i]|-m_r)^2]^2}\right| \tag{7}$$

$$S=\left|\frac{E[(|r[i]|-m_r)^3]}{E[(|r[i]|-m_r)^2]^{\frac{3}{2}}}\right| \tag{8}$$

$$PSD=\frac{1}{N}\max|DFT(r_{cn}[i])|^2 \tag{9}$$

$$PRR=\frac{\max(|r(:)^2|)}{\frac{1}{N}\sum_{i=1}^{N}(r[i])^2} \tag{10}$$

$$PAR=\frac{\max(|r(:)|)}{\frac{1}{N}\sum_{i=1}^{N}(r[i])} \tag{11}$$

where N is the number of samples for signal data, E[·] is the expectation computation, max(·) is the maximum of the received signal r[i] and r(:) represents all samples of the received signal r[i].

All above statistical features were chosen to classify the modulated signal dataset. The process of feature extraction is automatically realized by artificial design and statistical knowledge in our model.

III. RESULTS AND DISCUSSION

The dataset is stored in hdf5 format, with 2,555,904 examples, each 1024 samples in length. These samples are uniformly distributed in SNR from -20dB to +30dB and tagged so that we can evaluate performance on specific subset.

Authorized licensed use limited to: INSTITUTO MILITAR DE ENGENHARIA. Downloaded on April 12,2025 at 16:59:36 UTC from IEEE Xplore. Restrictions apply.

We use approximately 2000,000 examples for training, and 500,000 examples for testing and validation. The training and testing process are accelerated by NVIDIA GeForce GTX 1080Ti and the implementation of network is based on Keras with Tensorflow as the backend.

A. Overall Classification Performance

The overall correct classification probabilities of both baseline ResNet and HoS-based ResNet are plotted in Fig. 3. It can be seen that the overall correct classification probabilities can reach above 95% accuracy by around 10 dB, and it also outperforms the baseline ResNet. As a comparison, the correct classification probability of our ResNet improves 0.3%-6% than the baseline ResNet in the same condition of SNR and increases nearly 6% when SNR = 0 dB. Generally, the gap between the performance of two experimental results is gradually narrowed as the SNR increases, performance between HoS-based ResNet and baseline ResNet is virtually identical at high SNRs. But performance of HoS-based ResNet is less sensitive at lower SNRs, it, which shows roughly 2 dB lower sensitivity than the baseline ResNet for equivalent classification accuracy. We speculate that our ResNet is more suitable for synthetic impairments and relatively stable on overall classification accuracy after combining the statistical features.

As shown in Fig. 4, the x-axis is the epoch of training process, and the y-axis is the training loss. The loss curves of BL ResNet and HoS-based ResNet are plotted with different colors. We can notice that the loss decreases gradually with the increase of epoch. The training loss drops sharply at the beginning and then descends steadily. When loss is higher than 1.9, the loss of two networks tends to be similar and does not obviously decrease with the increase of epoch. We speculate that HoS-based model extracts essential features of signal data to accelerate the convergence of training process.

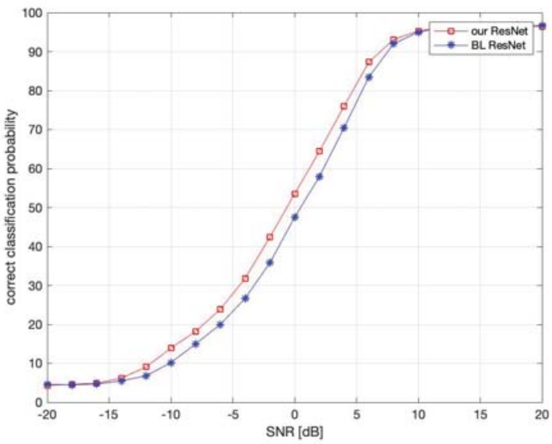

Fig. 3 The overall correct classification probability

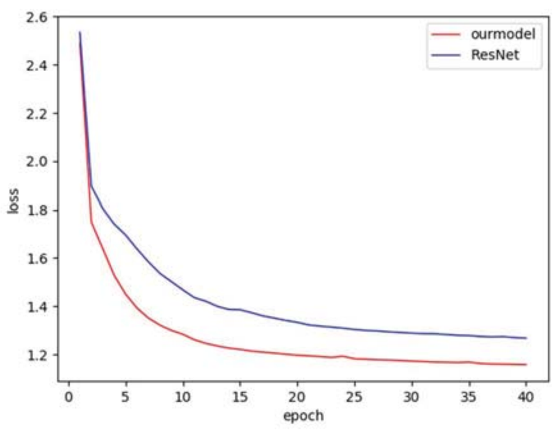

Fig. 4 The loss curves of different networks

B. Performance of Different Modulation Types

To further study the correct probability performance, the confusion matrices of two ResNets are visualized in Fig. 5 and Fig. 6 at the region of SNR = 4 dB and SNR = 10 dB, respectively. These confusion matrices help us analyze how precisely the classifiers perform on individual modulation type. Each column represents the predicted modulation type, and each row denotes the true label of modulated signal.

From Fig. 5, we can see that the largest sources of error are between high order quadrature amplitude modulations as well as between AM modes (confusing with-carrier (WC) and suppressed-carrier (SC)). Specifically, HoS-based ResNet shows more remarkable performance improvement on 16/32QAM than the baseline ResNet. As shown in Fig. 6, the correct classification accuracy of 64/128/256 QAM using HoS-based ResNet is obviously higher than that of baseline ResNet when SNR = 10 dB.

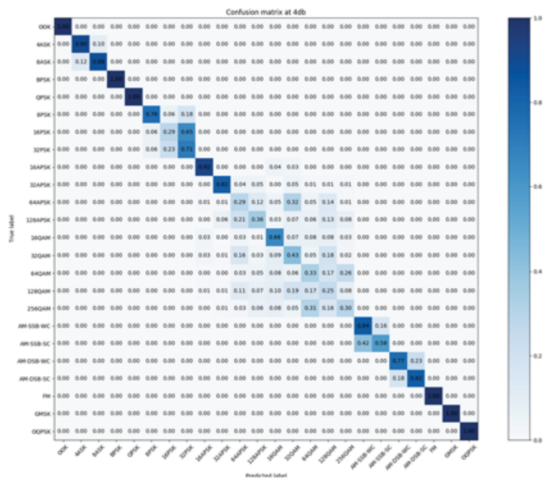

a. Baseline ResNet with SNR = 4dB

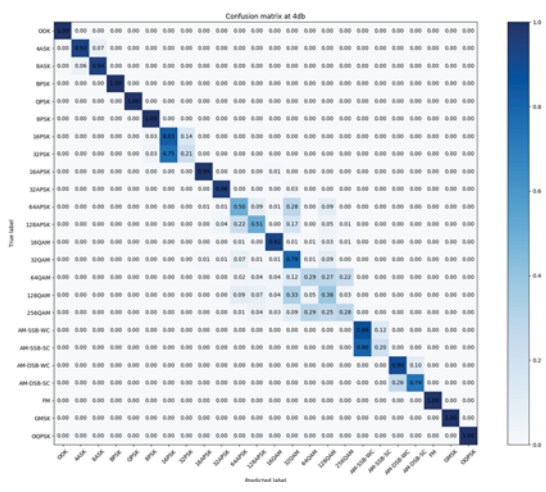

b. HoS-based ResNet with SNR = 4dB

Fig. 5 The 24-modulation confusion matrix for Baseline ResNet and HoS-based ResNet with SNR = 4dB

Authorized licensed use limited to: INSTITUTO MILITAR DE ENGENHARIA. Downloaded on April 12,2025 at 16:59:36 UTC from IEEE Xplore. Restrictions apply.

By comparing Fig. 5 and Fig. 6, we can notice that our proposed model achieves robust recognition performance on overall modulation types expect for high order modulations, even though SNR = 4dB. We speculate that HoS-based ResNet can fully dig out the signal information in the lower signal-to-noise ratio. We can also find that signals with lower information rates and notable features such as FM and 2/4/8ASK modulations are much more readily identified at low SNR, while high-order modulations require higher SNRs for better performance. We suppose it is largely due to the short time observations and changeable channel impairments, high-order QAMs and AM modes are easily mistakenly classified with its high information density.

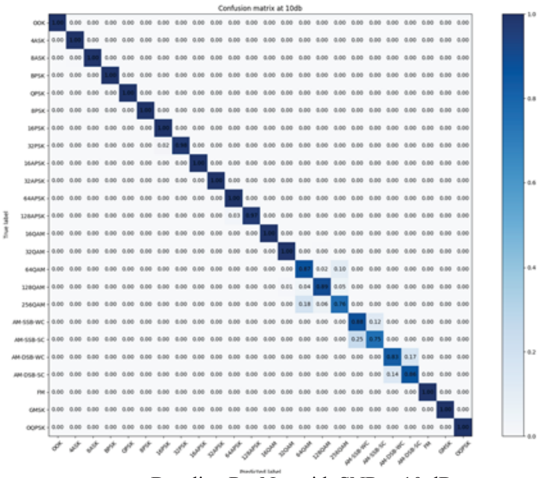

a. Baseline ResNet with SNR = 10 dB

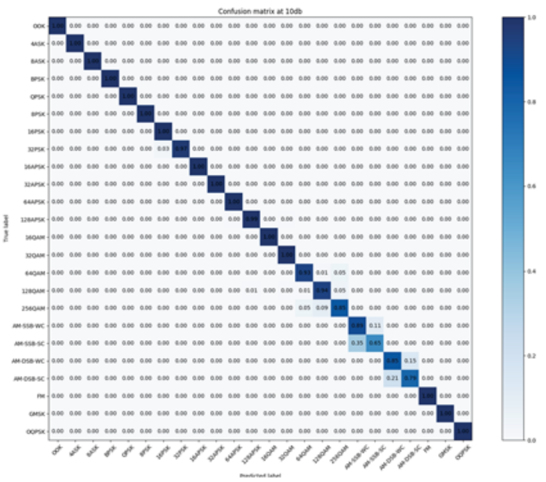

b. HoS-based ResNet with SNR = 10dB

Fig. 6 The 24-modulation confusion matrix for Baseline ResNet and HoS-based ResNet with SNR = 10 dB

IV. CONCLUSION

Deep neural network continues to show enormous promise in improving wireless signal identification accuracy, especially for real propagation effects and short-time observations. In this paper, we explore to combine higher-order statistics for generating features in the task of automatic classification and recognition. The novelty of this algorithm is that we propose a feature extraction scheme by concatenating HoS-based statistical features and DL-based representation features. Our proposed method can recognize twenty-four modulation types under real propagation effects. Theoretical analysis and experimental results verify the encouraging anti-noise effect of the novel high-order statistic features. Results show that the performance of the proposed HoS-based method is better than the baseline method in a wide range of SNR, which indicates the resulting algorithm is effective for a wide range of real propagation scenarios. Also, the average probability of correct classification is higher than the baseline method at lower SNR, which indicates the dramatic performance improvement and enhanced robustness over the existing methods.

REFERENCES

[1] T. O'Shea and J. Hoydis, "An Introduction to Deep Learning for the Physical Layer," in IEEE Transactions on Cognitive Communications and Networking, vol. 3, no. 4, pp. 563-575, Dec. 2017.

[2] T. J. O'Shea, T. Roy and T. C. Clancy, "Over-the-Air Deep Learning Based Radio Signal Classification," in IEEE Journal of Selected Topics in Signal Processing, vol. 12, no. 1, pp. 168-179, Feb. 2018.

[3] J. B. Tamakuwala, "New Low Complexity Variance Method for Automatic Modulation Classification and Comparison with Maximum Likelihood Method," 2019 International Conference on Range Technology (ICORT), Balasore, India, 2019, pp. 1-5.

[4] Gao L, Zhang X, Gao J, You S. Fusion Image Based Radar Signal Feature Extraction and Modulation Recognition[J]. IEEE Access, 2019:1-1.

[5] Wang Y, Liu M, Yang J, Gui G. Data-Driven Deep Learning for Automatic Modulation Recognition in Cognitive Radios[J]. IEEE Transactions on Vehicular Technology, 2019, 68(4):4074-4077.

[6] J. H. Lee, K. Kim and Y. Shin, "Feature Image-Based Automatic Modulation Classification Method Using CNN Algorithm," 2019 International Conference on Artificial Intelligence in Information and Communication (ICAIIC), Okinawa, Japan, 2019, pp. 1-4.

Authorized licensed use limited to: INSTITUTO MILITAR DE ENGENHARIA. Downloaded on April 12,2025 at 16:59:36 UTC from IEEE Xplore. Restrictions apply.